Effects of dilution on the magnetic ordering of a two-dimensional lattice of dipolar magnets

2005 J. Phys.: Condens. Matter 17 2137

(http://iopscience.iop.org/0953-8984/17/13/012)

INSTITUTE OF PHYSICS PUBLISHING JOURNAL OF PHYSICS: CONDENSED MATTER

J. Phys.: Condens. Matter **17** (2005) 2137–2147 doi:10.1088/0953-8984/17/13/012

Effects of dilution on the magnetic ordering of a two-dimensional lattice of dipolar magnets

S M Patchedjiev[1], J P Whitehead[1,3] and K De'Bell[2]

[1] Department of Physics and Physical Oceanography, Memorial University of Newfoundland, St John's, NF, A1B 3X7, Canada
[2] Department of Mathematical Sciences, University of New Brunswick at Saint John, Saint John, NB, E2L 4L5, Canada

Received 24 January 2005, in final form 25 February 2005
Published 18 March 2005
Online at stacks.iop.org/JPhysCM/17/2137

Abstract

Monte Carlo simulations are used to study the effects of dilution by random vacancies on the phenomenon of order arising from disorder in an ultrathin magnetic film. At very low concentrations of vacancies, both the collinear ordered phase observed in the undiluted system and the microvortex state are observed, and the boundary on which the reorientation transition between these states occurs is found to be consistent with the predictions of earlier work. However, even at vacancy densities as low as 0.5% there is evidence that the vacancies result in a energy landscape with a number of very nearly degenerate minima.

1. Introduction

The manner in which the interaction between disorder and frustration determine the properties of materials remains a subject of considerable interest and this has been studied in the context of a wide range of physical systems including the magnetic properties of pyrochlores [1] and molecular solid glasses [2]. In this paper we study the combined effects of structural and thermal disorder in an inherently frustrated system, an ultrathin film of magnetic dipoles.

In a previous study Henley and Prakash used spin wave theory and scaling arguments to study this problem for a truncated dipolar interaction which included only the nearest neighbour interaction [3–5]. In the case of both the square and the hexagonal lattice they concluded that, while the ground state of the system is a continuous manifold of degenerate states, thermal disorder breaks the degeneracy and results in ordered states in which the moments are aligned along the lattice axes in the case of the square lattice (collinear phase), an example of order coming from disorder [6]. Using a combination of spin wave theory and Monte Carlo simulations, a similar result was later confirmed in a model with a full dipolar interaction [7, 8]. Henley and Prakash also predicted that, at zero temperature, the introduction of structural

[3] Author to whom any correspondence should be addressed.

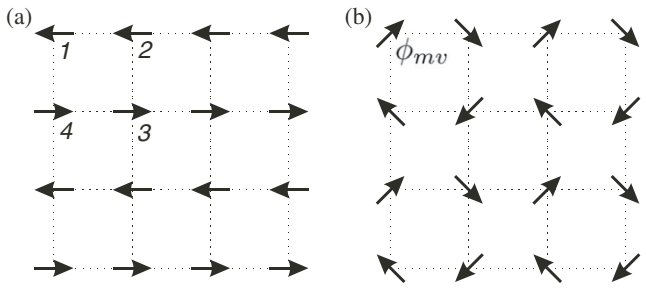

Figure 1. Two ground state spin configurations: (a) the collinear state with $\phi_{\rm mv} = \pi$ and (b) the microvortex with $\phi_{\rm mv} = \pi/4$.

disorder in the form of vacancies would also destroy the degeneracy of the ground state, resulting in a ground state in which the spins are aligned, on average, at 45° to the lattice axis (microvortex phase). A more recent study examined the effects of three types of structural disorder at zero temperature in two-dimensional nanostructure arrays [9], including disorder due to vacancies as discussed by Henley and Prakash.

In this study we consider a two-dimensional square lattice of magnetic dipoles constrained to lie in the plane of the lattice but free to rotate within it. The Hamiltonian of the system is given by

$$H = g \sum_{i \neq j} \left(\frac{\vec{\sigma}_i \cdot \vec{\sigma}_j}{r_{ij}^3} - 3 \frac{(\vec{\sigma}_i \cdot \vec{r}_{ij})(\vec{\sigma}_j \cdot \vec{r}_{ij})}{r_{ij}^5} \right). \tag{1}$$

The spins $\{\vec{\sigma}_i\}$ are treated as classical vectors of fixed length located at the sites of the lattice $\{i\}$ and confined to the plane of the lattice. We assume $g = 1$.

The ground states for this system form a degenerate manifold, characterized by the microvortex (MV) angle $\phi_{\rm mv}$ [9], as shown in figure 2 of [10], and which consist of a plaquette of four neighbouring spins aligned relative the x-axis with $\phi_1 = \phi_{\rm mv}$, $\phi_2 = -\phi_{\rm mv}$, $\phi_3 = \pi + \phi_{\rm mv}$, $\phi_4 = \pi - \phi_{\rm mv}$. Of particular interest are the collinear state ($\phi_{\rm mv} = n\pi/2$) shown in figure 1(a) and the microvortex phase ($\phi_{\rm mv} = (n + 1/2)\pi/2$) shown in figure 1(b).

It is sometimes convenient to represent the spin configurations in terms of the spin variables $\vec{S}(\vec{r})$, which are related to the original set of spin variables $\vec{\sigma}(\vec{r})$ by means of the transformation

$$S^x(\vec{r}) = (-1)^{n_y} \sigma^x(\vec{r}) \tag{2}$$

$$S^y(\vec{r}) = (-1)^{n_x} \sigma^y(\vec{r}) \tag{3}$$

where n_x and n_y denote the x and y lattice coordinates of the spin variables measured relative to some arbitrary origin. The ground state configurations, shown in figure 1 in terms of the original spin variables $\vec{\sigma}_j$, are shown in figure 2 in terms of the transformed spin variables $\vec{S}$. The merit of the transformation defined by equations (2) and (3) is that it maps each of the ground state spin configurations onto an equivalent ferromagnetic state aligned at an angle $\phi_{\rm mv}$ to the x-axis. This transformation proves useful as it helps us to visualize a particular spin configuration in terms of the transformed spins.

In this study we examine the effect of vacancies on the magnetic properties of a system of dipolar spins on a square lattice at finite temperature. Results are reported for lattice sizes of $N = 16 \times 16$, 32×32 and 64×64. Periodic boundary conditions are imposed on the spin configurations by constructing an infinite plane from replicas of the finite system. The summations of the dipolar interactions over the replicas are evaluated using the Ewald summation technique [11]. The simulations are carried out using the standard Metropolis

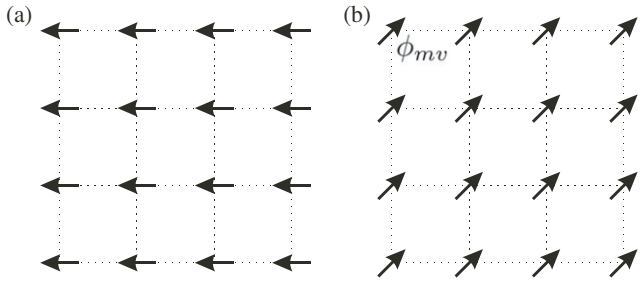

Figure 2. The ground state spin configurations corresponding to those in figure 1, but shown in the transformed spin variables defined by equations (2) and (3).

algorithm. For the results reported in the current work an equilibration time of 5×10^4 Monte Carlo steps per site (MCS/site) was used for each simulation. The number of samples used to calculate the averages for the two larger lattices was 75×10^4 MCS/site, using samples taken every 15 MCS/site. For the smaller lattice size the respective numbers were 10×10^5 MCS/site and 20 MCS/site.

We initially consider very low concentrations of vacancies and compare the Monte Carlo results with the predictions of Prakash and Henley [4]. We then turn our attention to the effect that increasing the concentration of vacancies has on the energy landscape of the system and the resulting complications from non-equilibrium effects.

2. Low vacancy concentrations

At finite temperature the magnetic character of the equilibrium phase may be expressed in terms of a conjugate field P defined as [7]

$$P(T) = \frac{1}{N}\left\langle \sum_{\vec{R}} \left(\sigma_x^4 + \sigma_y^4\right)\right\rangle. \tag{4}$$

A random orientation of the spins yields a value $P = 0.75$, while the collinear phase and the microvortex phase yield values of $P = 1.0$ and 0.5 respectively. De'Bell *et al* has shown that a system of dipolar spins on a square lattice has a continuous transition at $T = 1.4$ [7] from the high temperature paramagnetic phase to the low temperature collinear phase. This is reflected in the value of the conjugate field, which increases monotonically with decreasing temperature, from a value of $P = 0.75$ at high temperature to a value of $P = 1$ at $T = 0$.

In figure 3 we plot the conjugate field P obtained from ten separate Monte Carlo runs as a function of temperature for the case of $c = 0.37\%$, or 15 vacancies on a unit cell of 64×64. Each run has the same spatial distribution of vacancies on the lattice but uses a different seed to generate the Markov chain. Results are presented for both heating and cooling. While the data presented in figure 3 show that each individual run exhibits a relatively well defined transition from the collinear phase ($P \approx 1.0$) to the microvortex phase ($P \approx 0.5$) over a relatively narrow temperature range, the combined data for all the runs show a much broader range in temperature at which the transition occurs. This spread in the temperature range over which the transition occurs masks a small but discernible hysteresis on heating and cooling. The fact that in figure 3 the conjugate field, P, is somewhat less than its saturation value in the collinear phase simply reflects the local disorder created by the vacancies.

Further evidence regarding the nature of the transition is shown in figure 4 which shows histograms of the distribution of angles for two spin configurations generated at two

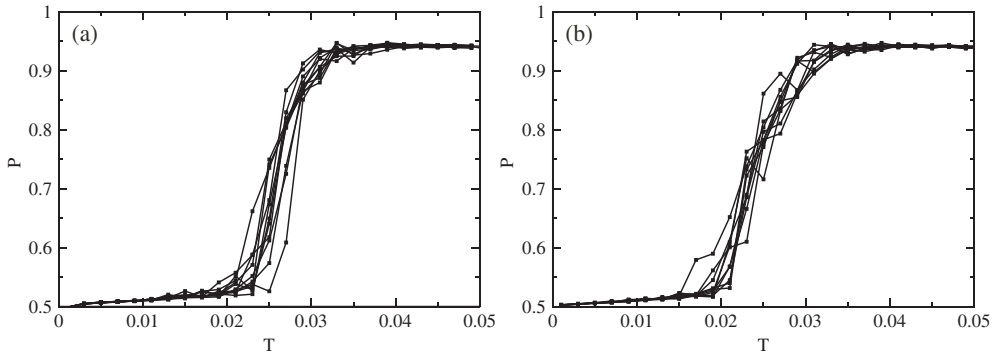

Figure 3. The conjugate field P plotted as a function of temperature for $c = 0.37\%$ (15 vacancies) for ten simulations with the same vacancy configuration but different Monte Carlo seeds. Results are shown for both heating (a) and cooling (b). The size of the unit cell is 64×64.

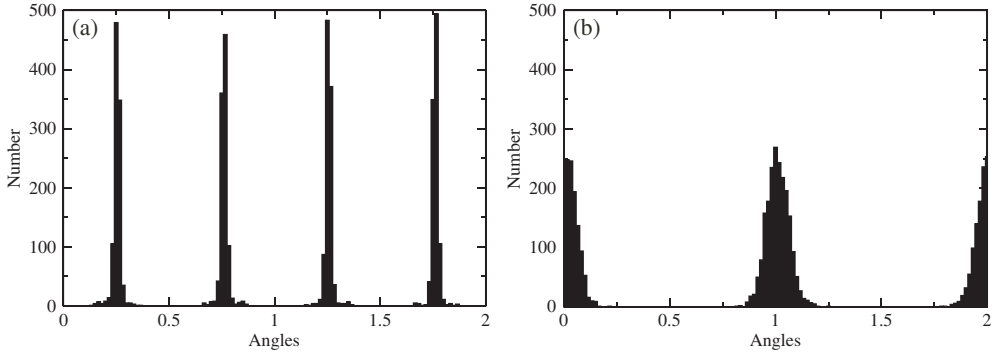

Figure 4. Histogram of the angular distribution of orientation angles, in units of π, for a single spin configuration for a vacancy concentration $c = 0.37\%$ (15 vacancies) for (a) $T = 0.001$ and (b) $T = 0.05$. The size of the unit cell is 64×64.

temperatures: $T = 0.05$ and 0.001. For $T = 0.05$ the angular distribution of the spins in figure 4(b) shows two peaks at 0 and $\pi/2$, corresponding to a collinear state with $\phi_{\mathrm{mv}} = 0$. On the other hand for $T = 0.001$ the angular distribution of the spins in figure 4(a) shows four peaks at $\pi/4$, $3\pi/4$, $5\pi/4$ and $7\pi/4$, corresponding to the microvortex state. The width of the peaks reflects the effects of thermal disorder and the fact that around the vacancies the spins point along directions other than the ones determined by the global MV angle.

In figure 5 the results of another ten Monte Carlo runs are presented for $c = 0.37\%$ or 15 vacancies on a unit cell of 64×64. In this case, each run was generated using a different random configuration of vacancies as well as a different seed. For each vacancy configuration the data exhibit a clear transition between the collinear and microvortex states. However, the spread in temperatures at which this transition occurs for the different runs is greater than the corresponding spread in the data shown in figure 3, in which the vacancy configuration is the same for each run.

In order to determine the phase transition for different vacancy concentrations we first average over several MC simulations with different initial seeds and then over at least five different vacancy configurations with the same number of vacancies. In figure 6 the resulting averaged curves for concentrations in the range of $c = 0.12$–0.46% are shown. The curves

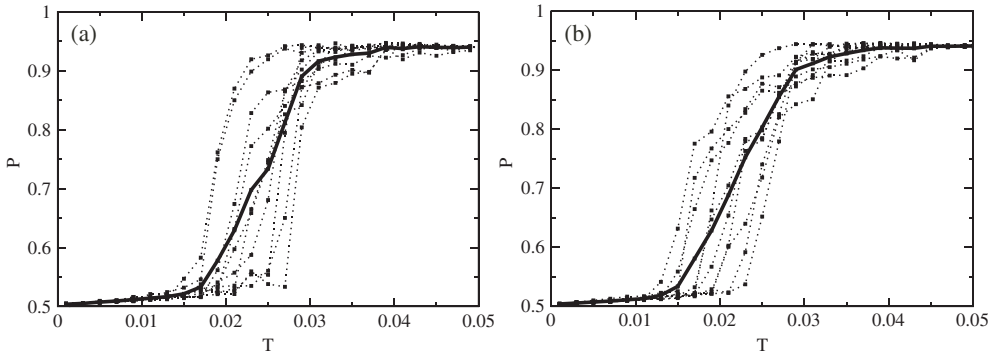

Figure 5. The conjugate field P plotted as a function of temperature for ten separate Monte Carlo runs for a vacancy concentration $c = 0.37\%$ (15 vacancies). Each run has a different vacancy configuration. The solid curve shows the conjugate field P averaged over the ten runs. The size of the unit cell is 64×64. Results are shown for both heating (a) and cooling (b).

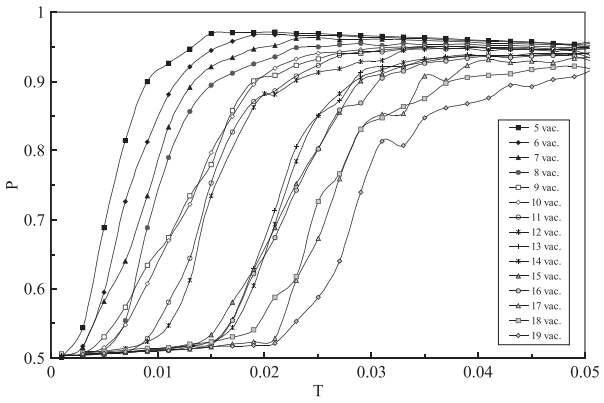

Figure 6. The conjugate field P plotted as a function of temperature for different vacancy concentrations. The values plotted are averaged over multiple Monte Carlo runs with different vacancy configurations. The size of the unit cell is 64×64. The concentration varies from $c = 0.12\%$ to 0.46% (5–19 vacancies).

show a clear trend in which the temperature at which the transition from the collinear to the microvortex phase occurs increases with increasing vacancy concentration.

In order to make a more quantitative study of this trend we define the transition temperature for each simulation as that temperature at which the value of P lies halfway between the maximum and minimum values. The resultant phase boundary separating the collinear and the microvortex states is shown in figure 7. The data indicate a linear dependence of the transition temperature on the concentration. A regression analysis yields the following relation between the transition temperature and the concentration: $T = (5.86 \pm 0.13)c$. This result compares with the slope of 5.75 obtained by Prakash and Henley for the truncated dipole-like interaction using linear spin wave theory [5].

At concentrations lower than $c \approx 0.1\%$ the perturbations on the system are so small that most of the simulations fail to show the transition to the microvortex state. As the temperature is lowered, P continues to rise monotonically to 1, and the system remains in the collinear state.

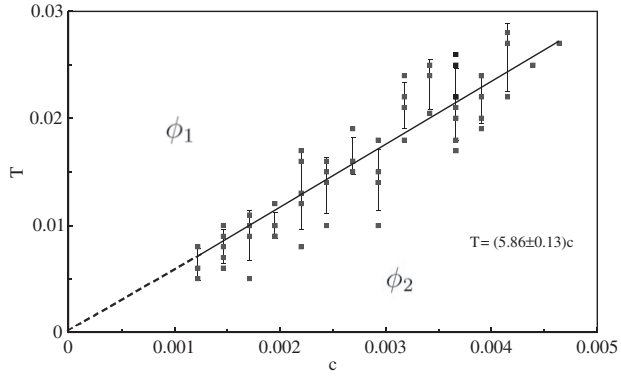

Figure 7. The phase boundary separating the collinear and the microvortex phase, for low values of the vacancy concentration $c < 0.5\%$. The size of the unit cell is 64×64. ϕ_1: collinear phase, ϕ_2: microvortex phase. Individual data points (black squares) correspond to different vacancy configurations and are included to indicate the spread around the mean.

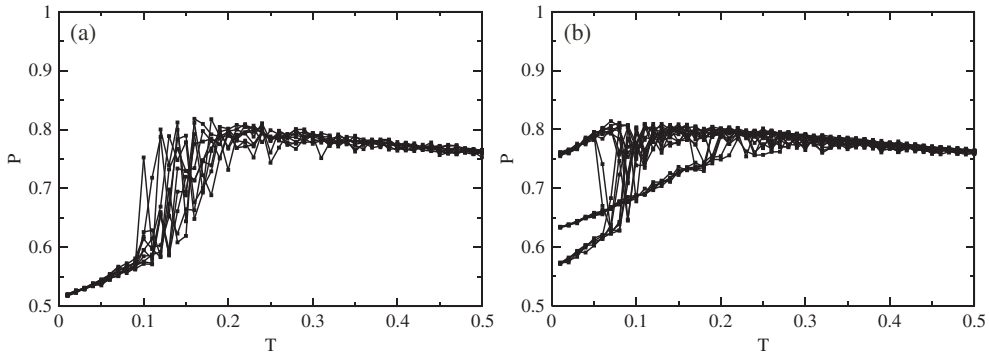

Figure 8. The conjugate field P plotted as a function of temperature on cooling for $c = 2.3\%$ (six vacancies). The size of the unit cell is 16×16. (a) The results from ten MC simulations with different initial seeds for the vacancy configuration shown figure 9(a). (b) The results from twenty MC simulations with different initial seeds for the vacancy configuration shown in figure 9(b).

3. Higher vacancy concentrations

For concentrations greater than 0.5% the spatial distribution of the vacancy configuration becomes significant in determining the response of the system to heating and cooling. Most significantly, at higher concentrations of vacancies, many of the MC simulations do not show a clear transition to the microvortex state on cooling. As an example we show the results from two simulations with $N = 16 \times 16$ and $c = 2.3\%$.

Figure 8 shows simulations for the two specific configurations of vacancies, presented in figures 9(a) and (b). For the vacancy configuration shown in figure 9(a), the results are qualitatively similar to those obtained for the lower vacancy concentrations, with the system relaxing to a single microvortex ground state on cooling in all of the ten simulations. The final state is shown in figure 9(a) in terms of the transformed variables defined by equations (2) and (3).

The second vacancy configuration, shown in figure 9(b), leads to a different MC evolution. In this case the system does not relax to the unique state on cooling. Instead the simulations

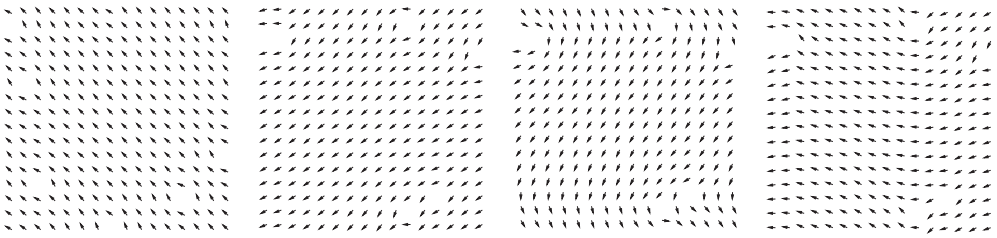

Figure 9. Final spin configurations at zero temperature obtained from MC simulation by cooling from the high temperature collinear phase. Results are shown for two separate vacancy configurations with $c = 2.3\%$ (six vacancies) on a 16×16 unit cell. (a) shows the final spin configuration for the first vacancy configuration, while (b)–(d) show the final spin configuration for the second. The temperature dependence of the conjugate field P corresponding to the vacancy configuration in (a) is shown in figure 8(a). The corresponding plot of the final spin configurations, corresponding to those presented in (b)–(d), is shown in figure 8(b). The energies of each configuration in units of g are included below the corresponding figure.

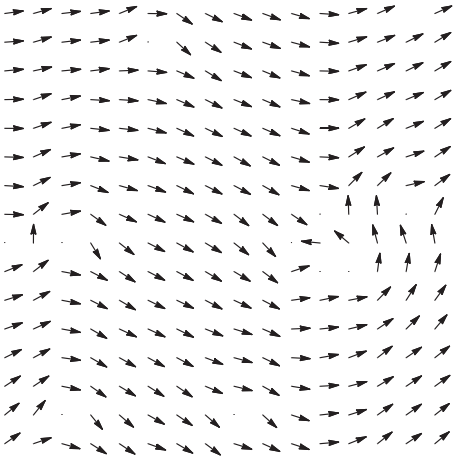

Figure 10. A 16×16 segment of the one of the zero-temperature configurations for a 32×32 lattice with $c = 2.9\%$ (30 vacancies).

show the system relaxing to one of the three different final states shown in figures 9(b)–(d) again in terms of the transformed spin variables. More significantly, of the three final states, the lowest energy state at $T = 0$ is not the state with the lowest value of the P shown in figure 9(b) ($P = 0.56$), corresponding to the microvortex state. Instead the ground state spin configuration is shown in figure 9(c) ($P = 0.63$) and cannot be readily characterized in terms of a single MV angle. Obviously, in this case, the energy surface at zero temperature has at least three distinct minima, one of which is the ground state, and the system locks into one of these three states as it is cooled. The relative difference of the energies of these states is small, of the order of 0.05%.

As the vacancy concentration is increased, the number of metastable spin configurations multiplies. In many cases the spins form domains as the temperature is decreased, each of which is characterized by a different local MV angle $\phi_{\mathrm{mv}} \approx (n + 1/2)\pi/2$. An example of a quarter of the lattice unit cell of such a final metastable state for a 32×32 lattice is given in figure 10.

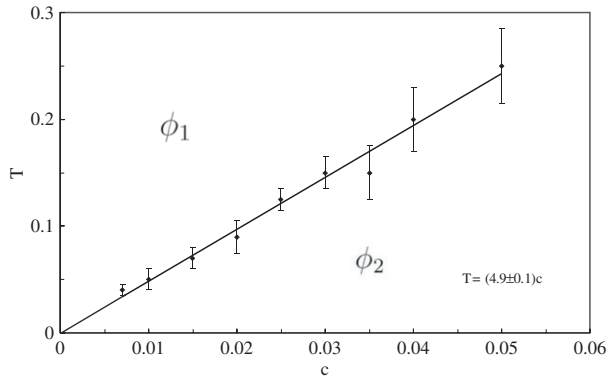

Figure 11. The phase boundary separating the collinear and the microvortex phase, extended to include higher values of vacancy concentration $c < 5.0\%$. The size of the unit cell is 64×64. ϕ_1: collinear phase, ϕ_2: microvortex phase.

Despite the complications arising from these metastable states for larger vacancy concentration, we can still usefully define a transition temperature as the temperature at which P is halfway between its minimum and maximum values, up to a concentration $c \approx 5\%$, even though the final state is not always a pure microvortex state. This allows us to extend the phase diagram to higher concentrations.

In figure 11 we present data for $N = 64 \times 64$ and concentrations from 0.7% to 5%. For the higher concentrations, determining exactly where the transition occurs becomes increasingly difficult for the reasons described above. Nevertheless there is still a clear linear trend with $T = (4.9 \pm 0.1)c$. The slope is close to but significantly less than the value obtained for lower concentrations and the value obtained by Prakash and Henley [5]. We believe this difference in the slope may be attributed, in part, to the curvature of the phase boundary. However, the variability of the data and the complications introduced by the metastable spin configurations with increasing vacancy concentrations preclude a quantitative determination of the degree of curvature in the phase boundary.

4. Angular distributions

In [9] Jensen and Pastor present an analysis of the role of vacancies in determining the distribution of minimum energy states for the present model. In their analysis they consider only those spin configurations in which the spins are perfectly correlated and can therefore be completely specified by a single MV angle, ϕ_{mv}. A total of 1000 different random vacancy configurations were sampled. For each configuration the value of the MV angle that minimized the energy of the system was obtained using a conjugate gradient method.

In the present work a procedure similar to that of Jensen and Pastor was used for the same periodic boundary condition system as was used in the Monte Carlo simulations. As in [9], only those spin configurations in which the spins are perfectly correlated are considered. A quadratic interpolation was used to minimize the total energy. A histogram showing the distribution of MV angles ϕ_{mv} obtained from the energy minimization is presented in figure 12 for a vacancy concentration of $c = 2.0\%$ on a 16×16 system. This graph is analogous to figure 6(a) in [9]. Due to the periodicity and equivalence of $\phi_i \rightarrow \phi_i + \pi$, only MV angles from 0 to π are presented.

The results obtained are consistent with those of [9] and show a peak corresponding to the microvortex states with $\phi_{\mathrm{mv}} = \pi/4$ and $3\pi/4$, as well as the collinear state with $\phi_{\mathrm{mv}} = 0$

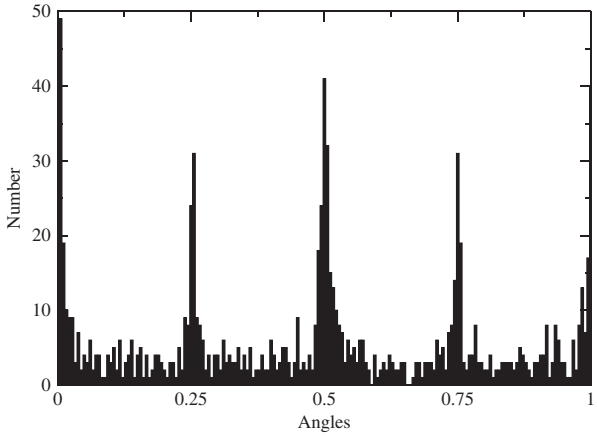

Figure 12. The distribution of microvortex angles ϕ_{mv} that minimizes the energy for different random vacancy configurations for $c = 2.0\%$ (five vacancies per unit cell), in units of π. The size of the unit cell is 16×16. Data show results from 1000 randomly selected vacancy configurations. Due to mirror symmetry, we only show the angular distribution for $0 \leqslant \phi_{mv} \leqslant \pi$.

and $\phi_{mv} = \pi/2$. For concentrations between $c = 2.0\%$ and 10.0% the peaks associated with the microvortex state at $\phi_{mv} = \pi/4$ and $3\pi/4$ decrease with increasing vacancy concentration and vanish for $c \geqslant 7\%$. The peaks at $\phi_{mv} = 0$ and $\pi/2$, corresponding to the collinear states, however, persist for all the values of concentration considered in the present work.

While these results are consistent with those obtained by Jensen and Pastor, the presence of the peaks associated with the collinear state in figure 12 appears to contradict the earlier results of Henley and Prakash as well as the Monte Carlo results reported in the previous section. However, it should be noted that by constraining the spin configurations to those states characterized by a uniform MV angle we do not properly take into account the perturbing effect of the vacancies in determining the equilibrium spin configuration.

In order to examine the perturbing effect of the vacancies in more detail, we generalize the earlier work of Jensen and Pastor to include the effect of local deviations from a uniform MV angle introduced by the vacancies. We begin by determining the MV angle that minimizes the energy as described above. Using that as our initial spin configuration we then treat each spin as an independent variable and minimize the energy using a quadratic interpolation scheme involving all 16 spins. In the resulting final state most of the spins are aligned along a common MV angle, ϕ_{mv}, but with noticeable deviations in the neighbourhood of the defects. For small number of vacancies this procedure almost always finds the ground state of the system, equivalent to that obtained from Monte Carlo simulation.

From the results used to generate figure 12 we take 1000 final spin configurations and minimize their energy using the procedure described. The distribution of the resultant conjugate field values is presented in figure 13. For the vacancy concentration of $c = 2.0\%$ there are no peaks other than that for $P = 0.5$, corresponding to the microvortex state. The peak does not appear at the exact value of $P = 0.5$, as the total number of dipoles is less than 16×16, and some of the dipoles in the vicinities of vacancies are not aligned at angles corresponding to $\phi_{mv} = \pi/4$.

As shown in figure 12(b) a higher number of vacancies broadens and shifts the peak to higher values of P. However, there is still only one peak. The artefact of a peak at $P = 1$, corresponding to the collinear state, does not appear at all.

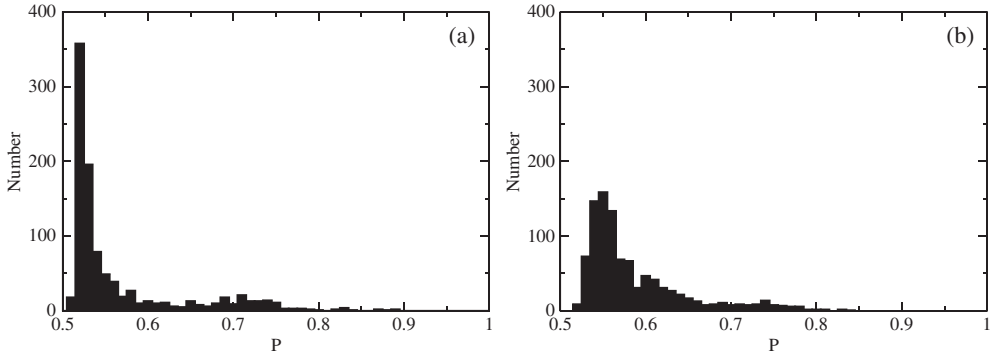

Figure 13. Histogram of the frequency distribution of the conjugate field P for 1000 different vacancy configurations. The size of the unit cell is 16×16. (a) $c = 2.0\%$ (5 vacancies per unit cell), (b) $c = 5.9\%$ (15 vacancies per unit cell).

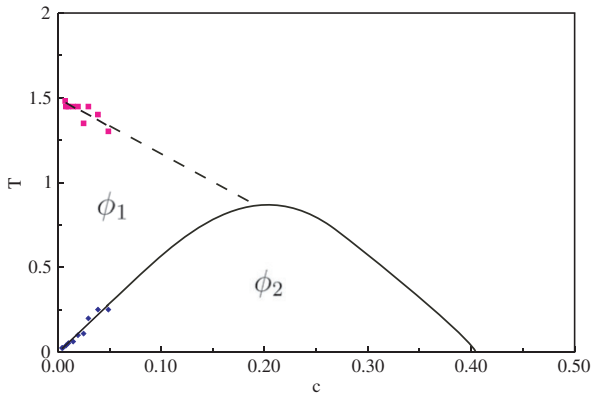

Figure 14. Points on the phase boundaries obtained from Monte Carlo simulation shown together with the $c-T$ phase diagram conjectured by Prakash and Henley [5]. ϕ_1: collinear phase, ϕ_2: microvortex phase.

(This figure is in colour only in the electronic version)

At still higher vacancy concentrations, it makes sense to adjust the normalization of P as $P' \to P/(1-c)$. Increasing the vacancy concentration does broaden the peaks even further and shifts them to higher values of P'. For $c = 50\%$ it is centred at $P' = 0.8$, reflecting a close to random distribution of dipole angles with respect to the axes.

5. Summary and phase diagram

In figure 14 we show our Monte Carlo simulation results for low concentrations of vacancies superimposed on the phase diagram conjectured by Prakash and Henley [4]. In addition to points on the phase boundary separating the collinear and the microvortex phase we also show points on the phase boundary separating the collinear and the paramagnetic phase. The locations of points on this boundary were determined from the peak in the specific heat. However, as the concentration of vacancies is increased the specific heat curve broadens and flattens, making the precise location of the phase boundary difficult to determine.

At very low concentrations of vacancies our results are consistent with those obtained by Prakash and Henley from spin wave theory for the truncated interaction model. Our results emphasize the importance of incorporating the deviations from the uniform microvortex state induced by the vacancies when determining the low energy states of the system. (Local small domain structures also play a role in determining the overall magnetic state in the case of regular arrays of vacancies ('antidots') in magnetic films; however, in this case the overall structure is periodic [12, 13].)

Our results also indicate that even concentrations of vacancies of $O(1\%)$ are sufficient to induce nearly degenerate local minima in the energy landscape. Amongst these nearly degenerate states, the lowest energy state is not necessarily the state that is magnetically closest to the microvortex state as one might suppose. An increasingly complex energy landscape, with many nearly degenerate minima and the corresponding difficulty in determining a clearly defined transition, suggests that it may not be useful or possible to characterize the system as a microvortex state even well below the percolation threshold for the system. This raises interesting questions regarding the appropriate description of the magnetic system at concentrations of vacancies between the very low values, where the description given by Prakash and Henley is accurate, and the percolation threshold.

Acknowledgments

This work was supported in part by the Natural Sciences and Engineering Research Council of Canada. The authors thank Jason Mercer for assistance with interpretation of the simulation data and the Memorial University of Newfoundland and University of the Calgary for the use of computational resources, provided under the auspices of C3.ca.

References

[1] Gardner J S, Ehlers G, Bramwell S T and Gaulin B D 2004 *J. Phys.: Condens. Matter* **16** S643–51
[2] Pilla S, Hamida J A, Muttalib K A and Sullivan N S 2001 *New J. Phys.* **3** 17.1–8
[3] Henley C 1987 *J. Appl. Phys.* **61** 3962
[4] Henley C 1989 *Phys. Rev. Lett.* **62** 2056–9
[5] Prakash S and Henley C L 1990 *Phys. Rev.* B **42** 6574–89
[6] Villain J, Bidaux R, Carton J P and Conte R 1980 *J. Physique* **41** 1263
[7] De'Bell K, MacIsaac A B, Booth I N and Whitehead J P 1997 *Phys. Rev.* B **55** 15108–18
[8] Rastelli E, Regina S, Tassi A and Carbognani A 2002 *Phys. Rev.* B **65** 94412
[9] Jensen P J and Pastor G M 2003 *New J. Phys.* **5** 68.168.22
[10] Abu-Labdeh A M, Whitehead J P, De'Bell K and MacIsaac A B 2002 *Phys. Rev.* B **65** 024434
[11] De'Bell K, MacIsaac A B and Whitehead J P 2000 *Rev. Mod. Phys.* **72** 225
[12] Cowburn R P, Adeyeye A O and Bland J A C 1997 *Appl. Phys. Lett.* **70** 2309
[13] Cowburn R P, Adeyeye A O and Bland J A C 1997 *J. Magn. Magn. Mater.* **173** 193